CLINICS

BASIC RESEARCH

Myeloid-derived suppressor cells and associated events in urethane-induced lung cancer

Daniela Teixeira,[I] Joaquim Soares de Almeida,[II] Bruna Visniauskas,[III] Guiomar Nascimento Gomes,[IV] Aparecida Emiko Hirata,[IV] Valquiria Bueno[I]

[I] Federal University of São Paulo (UNIFESP), Immunology Division, São Paulo/SP, Brazil. [II] Federal University of São Paulo (UNIFESP), Pathology Division, São Paulo/SP, Brazil. [III] Federal University of São Paulo (UNIFESP), Psychobiology Division, São Paulo/SP, Brazil. [IV] Federal University of São Paulo (UNIFESP), Physiology Division, São Paulo/SP, Brazil.

OBJECTIVES: Myeloid-derived suppressor cells contribute to the immunosuppressive microenvironment during tumor development and limit the efficacy of cancer immunotherapy. Identifying myeloid-derived suppressor cells and associated factors is the first step in creating strategies to reverse the suppressive effects of these cells on the immune system.

METHODS: To induce lung cancer, we administered 2 doses of urethane to BALB/c mice and observed these animals for 120 days. After this period, we evaluated the percentage of myeloid-derived suppressor cells in the blood, lung and bone marrow. The expression of alpha-smooth muscle actin, transforming growth factor-β, Toll-like receptor 2, Toll-like receptor 4, and interleukin-6 was also determined in the lung tissue.

RESULTS: Myeloid-derived suppressor cells were increased in all evaluated tissues after lung cancer development in association with increased Toll-like receptor 4 expression and decreased interleukin-6 expression in the lung. We observed alpha-smooth muscle actin and transforming growth factor-β expression in lung nodules.

CONCLUSIONS: We believe that the early diagnosis of cancer through determining the blood levels of myeloid-derived suppressor cells followed by the depletion of these cells should be further investigated as a possible approach for cancer treatment.

KEYWORDS: Lung Cancer; Myeloid-Derived Suppressor Cells; Toll-Like Receptors; Cytokines; Fibroblasts.

Teixeira D, Almeida JS, Visniauskas B, Gomes GN, Hirata AE, Bueno V. Myeloid-derived suppressor cells and associated events in urethane-induced lung cancer. Clinics. 2013;68(6):858-864.

Received for publication on November 14, 2012; **First review completed on** December 12, 2012; **Accepted for publication on** February 19, 2013

E-mail: valquiriabueno@hotmail.com

Tel.: 55 11 5549-6073

INTRODUCTION

Myeloid-derived suppressor cells (MDSCs) in mice are $CD11b^{+}Gr1^{+}$ cells with monocytic ($CD11b^{+}Gr1^{mid}Ly6G^{+/-}Ly6C^{high}CD49d^{+}$) and granulocytic ($CD11b^{+}Gr1^{high}Ly6G^{+}Ly6C^{neg}CD49d^{neg}$) characteristics (1). Recently, we demonstrated that there was a significant increase in lung-infiltrating cells 20 days after urethane injection in a urethane-induced lung cancer mouse model. Using flow cytometry, we observed that in control mice, less than 1% of the lung-infiltrating cells were $CD11b^{+}Gr1^{+}$; however, these cells accounted for 10% in mice with urethane-induced lung cancer (2). Other researchers have shown an increase in MDSCs during tumor development and their immunosuppressive role. The increased number of MDSCs in patients has been associated with metastasis and poor prognosis (3-5). Srivastava et al. showed that Lewis lung carcinoma (LLC) cells injected into C57BL/6 mice caused tumor growth in association with a significant increase in MDSCs. Treatment with anti-Gr1 or anti-Ly6G inhibited tumor volume, tumor weight, and metastases and reduced the number of cells expressing Gr1 in the tumor, blood, spleen and bone marrow. Moreover, anti-Gr1 treatment increased the frequency and function of effector NK and T cells (6).

MDSC activation is mediated by activated T cells and tumor stroma products, including IFN-γ, ligands for Toll-like receptors, IL-13, IL-4 and transforming growth factor-β (1). Recently, it was shown that tumor-infiltrating myeloid cells induce tumor resistance to cytotoxic T cells in mice and may contribute to the limited efficacy of cancer immunotherapy (7).

To better understand the mechanism through which MDSCs contribute to cancer development, we used a mouse model of urethane-induced lung cancer and evaluated the associated events.

No potential conflict of interest was reported.

DOI: 10.6061/clinics/2013(06)22

MATERIALS AND METHODS

Eight- to 10-week-old male BALB/c mice (bred in CEDEME/UNIFESP) were housed in cages and cared for in accordance with the Principles of Laboratory Animal Care (NIH publication 86-23, revised 1985) and the regulations of the Brazilian Committee on Animal Experimentation. The project was submitted to and approved by the Animal Ethics Committee of UNIFESP (protocol 0117/09).

Control mice were observed for 120 days.

Urethane mice were injected twice (i.p.) with 1.5 g/kg urethane (Sigma Chemical Company, St Louis, MO) dissolved in 0.9% NaCl, with an interval of 48 hours between administrations. These mice were observed for 120 days.

Mouse evaluation

After 120 days of follow-up, the BALB/c mice were anesthetized, and blood, lungs, and bone marrow were harvested. The percentage of $CD11b^{+}Gr1^{+}$ cells in these tissues was determined with flow cytometry. The lung lobes were sectioned and used for histology, immunohistochemistry and Western blot analysis.

Histological analysis

The lungs were fixed in 4% buffered formalin followed by paraffin embedding. The fixed lungs were cut into 4 μm sections, placed on glass slides, and stained with hematoxylin and eosin (H&E). These sections were then reviewed by a pathologist who was blinded to the procedures.

Nodule measurement

H&E-stained lung tissue was observed with an image system at 500x magnification. Each nodule was photographed, and Image Pro Plus 3.0 software was used to analyze the data. Briefly, a circle was drawn around the nodule with an electronic pen, and the area was immediately calculated with the UHTSCSA Image Tool 3.0.

Immunohistochemistry

Lung sections (5 μm) were deparaffinized in xylene, rehydrated in graded ethanol, and then pretreated in a microwave (Eletrolux, SP, Brazil) with 10 mM citric acid buffer (pH 6) for 3 cycles of 5 min each at 850 W for antigen retrieval. The sections were preincubated with 0.3% hydrogen peroxidase in PBS for 5 min to inactivate endogenous peroxidases and blocked with 5% normal goat serum in PBS for 10 min. The specimens were then incubated with an anti-smooth muscle alpha actin monoclonal antibody (α-SMA; clone 1A4: M0851, Santa Cruz Biotechnology, CA, USA) diluted 1:500. Another set of lung sections was incubated with anti-transforming growth factor-β monoclonal antibody (TGF-β1; sc-146, Santa Cruz Biotechnology, CA, USA) at 1:200. The incubation was performed overnight at 4℃ and followed by two washes in PBS for 10 min.

The sections were then incubated with anti-rabbit biotin-conjugated secondary antibody (Vector Laboratories, CA, USA) diluted at 1:200 in PBS for 1 h. The sections were washed twice with PBS followed by incubation with the preformed avidin biotin complex conjugated to peroxidase (Vector Laboratories, CA, USA) for 45 min. The bound complexes were visualized with 0.05% 3-3′-diaminobenzidine (DAB) solution.

Western blotting for TLR2, TLR4, and IL-6 protein

Solubilization buffer containing 100 mM Tris, pH 7.6, 1% Triton X-100, 0.01 mg/mL aprotinin, 2 mM PMSF, 10 mM Na_3VO_4, 10 mM NaF, 10 mM $Na_4P_2O_7$, and 10 mM EDTA was added to the lungs, and the organ was sonicated. The insoluble material was removed with centrifugation at 11,000 rpm at 4℃ for 30 min. The supernatant was used to measure the protein concentration (Bradford - ELISA assay). Protein expression was determined by loading samples (50 μg) onto a 10% SDS-polyacrylamide gel. The proteins were then electrotransferred from the gel to a nitrocellulose membrane for 90 min at 120 V. To reduce non-specific protein binding to the nitrocellulose membrane, the filter was pre-incubated overnight at 4℃ in blocking buffer (5% nonfat dry milk, 10 mM Tris, 150 mM NaCl and 0.02% Tween 20). The nitrocellulose membranes were incubated overnight at 4℃ with anti-TLR2, anti-TLR4 (Santa Cruz Biotechnology, CA, USA), and anti-IL-6 antibodies (R&D Systems) diluted in blocking buffer (3% nonfat dry milk, 10 mM Tris, 150 mM NaCl and 0.02% Tween 20). The membranes were then incubated with secondary antibody conjugated to horseradish peroxidase diluted in blocking buffer (1% nonfat dry milk, 10 mM Tris, 150 mM NaCl and 0.02% Tween 20) for 60 min. To visualize the proteins, enhanced chemiluminescence reagents were used, and the membranes were exposed to pre-flashed Kodak XAR film (Eastman Kodak, Rochester, NY). Quantitative analysis was performed with Scion Image software (Frederick, MD, USA).

Statistical analysis

The results are shown in graphical form as the mean ± standard error. A non-parametric Mann Whitney test was performed for group comparisons, and differences were considered significant at $p<0.05$.

RESULTS

The percentage of myeloid-derived suppressor cells ($CD11b^{+}Gr1^{+}$) was increased in the blood, lung and bone marrow of urethane-treated mice 120 days after cancer induction (Figure 1). Moreover, the absolute number of $CD11b^{+}Gr1^{+}$ cells was higher in the blood and lungs of mice from the urethane group compared to the control group. In urethane-treated mice, the area of the lung nodules ranged from 7998.90 mm^2 to 22595.76 mm^2, whereas the control mice had no lung nodules or hyperplasia (Table 1). Figure 2 shows α-SMA expression in the lung tissue. This marker is characteristic of differentiated myofibroblasts in tumor microenvironments but can also be expressed in vessels. Urethane-treated mice expressed α-SMA in the stroma and vessels of lung nodules (Figures 2C and 2D). Lungs from the urethane-treated mice exhibited higher TLR4 protein expression than the control group (control = 1.4 ± 0.7, urethane = 3.0 ± 0.6). TLR2 protein expression in lung tissue was similar between the groups (control = 0.74 ± 0.07, urethane = 0.72 ± 0.04), and IL-6 protein expression was decreased in the urethane-treated group (control = 0.61 ± 0.13, urethane = 0.21 ± 0.04; Figures 3A-C). TGF-β was strongly expressed in the lung bronchiole epithelium of mice in both the control and urethane groups. TGF-β expression was also observed in the lung nodules (Figure 4 A-D).

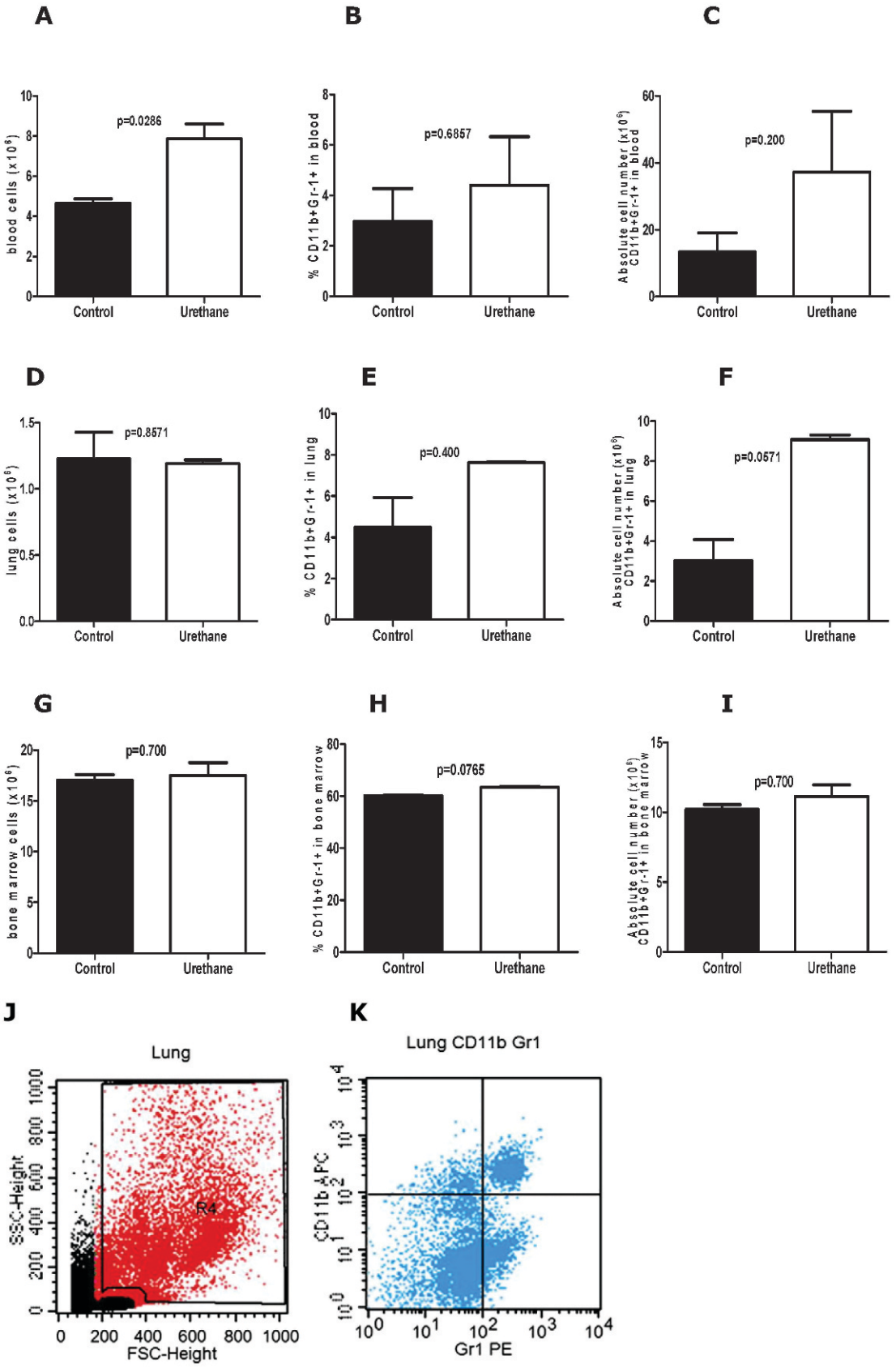

Figure 1 - Evaluation of BALB/c mice at 120 days after urethane (n = 4) injection *versus* the control (n = 4) mice. The urethane-treated mice showed an increase in the absolute cell number of $CD11b^{+}Gr\text{-}1^{+}$ cells (myeloid derived suppressor cells, MDSCs, p = 0.0571) in the lung and a higher percentage of MDSCs in the bone marrow (p = 0.0765). A representative dot plot of the flow cytometry results (**J, K**).

Table 1 - Evaluation of lung nodules in BALB/c mice. The control mice had no nodules and the urethane-treated mice had an average of 5 nodules after 120 days.

Groups	Number of nodules	Area of nodules
Control (n = 5)	0	0
Urethane (n = 5)	5.25 ± 0.96	14,570 ± 1,790 mm^2

DISCUSSION

Consistent with our previous results (2,8,9), all mice injected with urethane in this study developed lung nodules and showed an increase in MDSCs. The increase in MDSCs has been associated with immune system modulation that favors tumor growth. Notably, we observed that the control mice also presented with some MDSCs in the blood, lung, and bone marrow after 120 days (16-week-old mice) of follow-up. The lungs of the control mice contained 5.7% MDSCs, whereas our previous study showed that after 20 days (8- to 9-week-old mice) of follow-up, the control mice had less than 1% MDSCs in the lung (2). We hypothesize that this difference is because of ageing. This finding is consistent with Enioutina et al. (10), who showed an increase in $CD11b^{+}Gr1^{+}$ cells in the spleen, peripheral lymph nodes, bone marrow and blood of old mice compared with young mice. The increase in MDSCs because of the ageing process could contribute to the development of lung nodules after urethane administration.

Components of the microenvironment play an important role during tumor development. Tumor-infiltrating myofibroblasts facilitate tumor growth, invasion and metastasis by secreting growth factors and cytokines, and they also

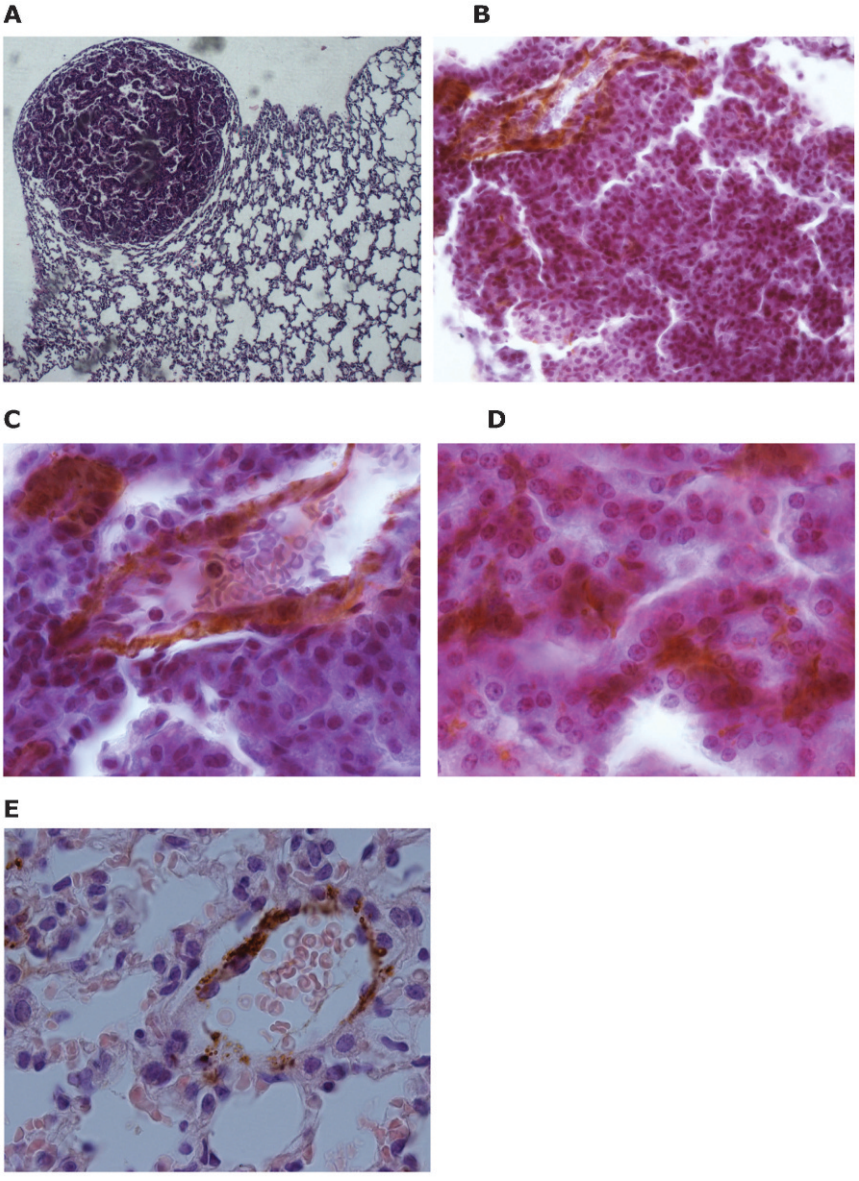

Figure 2 - Histology and immunohistochemistry performed on the lungs of BALB/c mice at 4 months after urethane administration. A representative lung from a urethane-treated mouse showing a nodule after 4 months of follow-up **(A,** 100x**)**. Global view of a lung nodule showing α-smooth muscle actin expression **(B,** 400x**)** and more detail of this expression in a vessel **(C,** 1000x**)** and tumor cell **(D,** 1000x**)**. Lung from a representative control mouse showing α-smooth muscle actin expression in a vessel **(E,** 1000x**)**.

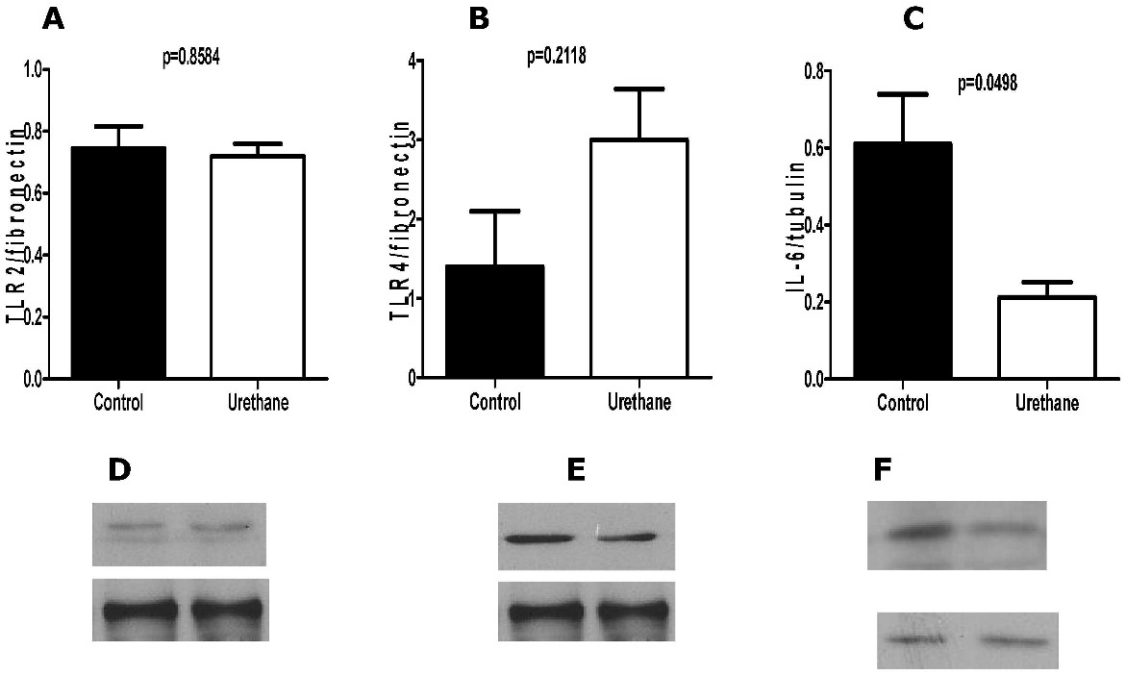

Figure 3 - Lung tissue from the control (n = 3) and urethane (n = 4) groups evaluated with western blotting for TLR2 **(A)**, TLR4 **(B)** and IL-6 **(C)** expression. TLR4 expression is increased in the lung from urethane-treated mice. IL-6 expression is higher in the lungs from control mice. A representative blot of each protein indicates the ratios of TLR2 and fibronectin **(D)**, TLR4 and fibronectin **(E)**, and IL-6 and tubulin **(F)**.

produce matrix and matrix-associated molecules (11-13). Horie et al. (14) observed that cultured fibroblasts from patients with resected lung cancer stroma (CAFs) had a higher expression of α-SMA than normal fibroblasts. Consistent with this finding, we observed α-SMA expression in the vessels and tumor stroma of urethane-treated

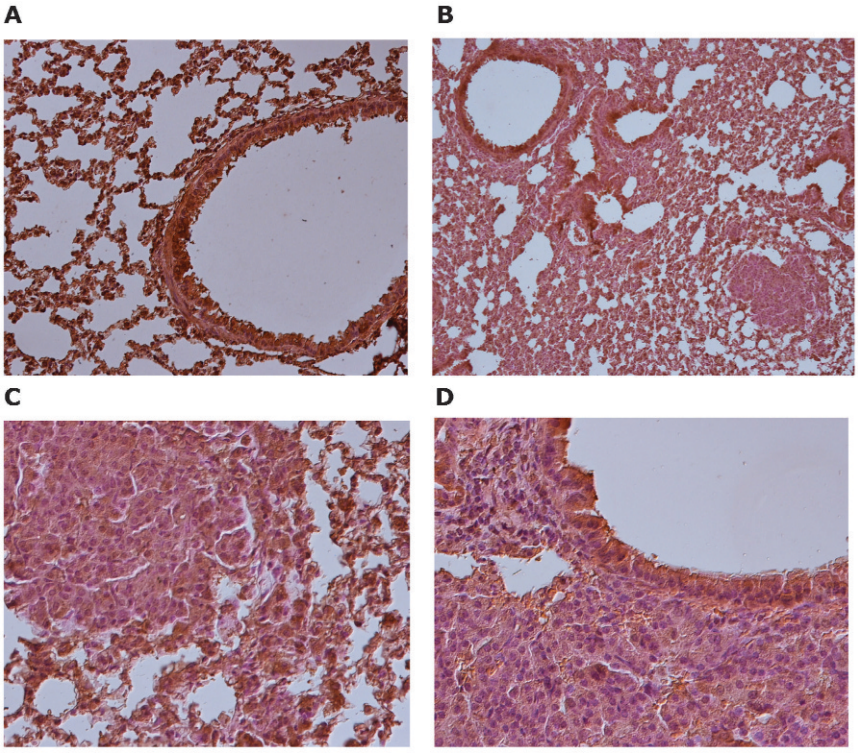

Figure 4 - Immunostaining of TGF-β in the lungs from control mice **(A,** 200x**)** showing intense positivity in the bronchiole epithelium, and lungs from urethane-treated mice showing positive staining in the bronchioles and nodule **(B,** 100x**)**. Details of the staining for TGF-β in the lung nodule **(C**, 400x**)** and bronchiole epithelium **(D,** 400x**)**.

mice, whereas in the control mice, α-SMA was expressed only in the vessels (Figure 2). Nazareth et al. (15) showed that fibroblasts from fresh lung tumor biopsy tissues produced TGF-β1 in the majority of samples tested (7 of 8), whereas only 2 tumor cell samples were positive for this marker, and the lymphocytes were negative. TGF-β1 has been implicated, at least in part, in the hyporesponsiveness of T cells in human non-small cell lung cancer (16). In our model, α-SMA expression in lung nodules suggests the presence of myofibroblasts, which may produce modulators that suppress the immune system and render the tumor microenvironment even more suppressive. Confirming our hypothesis, we observed TGF-β1 expression in the lung nodules of urethane-treated mice, whereas the bronchiole epithelium was positive for this marker in both the control and urethane-treated groups.

Tumor development is the result of several factors that act in the immune system (effectors *versus* suppressors). Inflammation regulates some of these factors and is associated with tumor growth. Bunt et al. (17) evaluated cells from BALB/c mice with 4T1 tumors stimulated with IL-1β to promote a pro-inflammatory microenvironment. BALB/c macrophages co-cultured with MDSCs and treated with both LPS and IFN-γ produced high levels of IL-10, even in the absence of MDSCs. Mice deficient in TLR4 produced no IL-10 and were not effective in reducing IL-12 production by macrophages. The authors concluded that TLR4 is a potential target for intervention in MDSC activation and immune system suppression. In a metastatic breast tumor model, Ahmed et al. (18) showed that the number of metastatic lung nodules was higher in $TLR4^{-/-}$ mice, whereas TLR4 knockdown in tumor cells (4T1) caused a relative reduction in lung metastasis. The authors concluded that TLR4 may play a defensive role at the level of the host and a negative role at the level of the cancer. Consistent with this finding, we observed that urethane-treated mice had higher levels of TLR4 at the tumor site (lung tissue) compared to the control mice. This finding was associated with a significant increase in the absolute number of $CD11b^{+}Gr1^{+}$ cells in the lungs of the urethane-treated group.

Notably, we found a significant decrease in IL-6 protein in lung tissue from urethane-treated mice compared to the control animals. IL-6 is both an inducer and a product of MDSCs (19); therefore, we expected to observe an increase in this cytokine after cancer development. However, because we did not measure IL-6 levels in the other sites, it is not possible to confirm whether this cytokine was increased in the serum or spleen cells. In addition, several reports have shown an increase in circulating IL-6 during cancer development (20,21).

Cheng et al. (22) showed an associative role for TLR4, IL-6, and TGF-β1 in tumor progression in human cervical cancer cells and HeLa cells. They observed TLR4 overexpression in cervical cancer cells, whereas HeLa cells treated with LPS showed TLR4 activation and developed anti-apoptotic and proliferative processes that were associated with IL-6 and TGF-β1 production. Bierie & Moses suggested that the regulation of tumorigenesis, including carcinoma initiation, progression and metastasis, by TGF-β signaling depends on its effects on both the tumor and host cell populations (23). Tumor-infiltrating myeloid-derived suppressor cells produce more TGF-β and play a suppressive role on host immune cells, thereby promoting tumor growth (24).

Srivastava et al. (6) showed that removing MDSCs from murine cancer improves antitumor immune responses and leads to significant tumor growth inhibition. In conclusion, we believe that the early diagnosis of cancer through determining the blood levels of myeloid-derived suppressor cells followed by the depletion of these cells should be further investigated as a possible approach for cancer treatment.

ACKNOWLEDGMENTS

This study was partially supported by Fundação de Amparo à Pesquisa do Estado de São Paulo (FAPESP). Bueno V received a fellowship from Conselho Nacional de Pesquisa (CNPq).

AUTHOR CONTRIBUTIONS

Teixeira D performed flow cytometry and contributed to writing the text. Almeida JS performed lung histology and contributed to writing the text. Visniauskas B and Novaes GN performed immunohistochemistry of the lung tissue and contributed to writing the text. Hirata AE performed the western blots of the lung tissue and contributed to writing the text. Bueno V performed the cancer induction, tissue harvesting, and statistical analysis and contributed to writing the text.

REFERENCES

1. Gabrilovich DI, Nagaraj S. Myeloid-derived-suppressor cells as regulators of the immune system. Nat Rev Immunol. 2009;9(3):162-74, http://dx.doi.org/10.1038/nri2506.
2. Rosin FC, Pedregosa JF, Almeida JS, Bueno V. Identification of myeloid-derived suppressor cells and T regulatory cells in lung microenvironment after Urethane-induced lung tumor. Int Immunopharmacol. 2011;11(7):870-5.
3. Diaz-Montero CM, Salem ML, Nishimura MI, Garret-Mayer E, Cole DJ, Montero AJ. Increased circulating myeloid-derived suppressor cells correlate with clinical cancer, metastatic tumor burden, doxorubicin-cyclosphosphamide chemotherapy. Cancer Immunol Immunother. 2009;58(1):49-59, http://dx.doi.org/10.1007/s00262-008-0523-4.
4. Yuan XK, Zhao XK, Xia YC, Zhu X, Xiao P. Increased circulating immunosuppressive CD14(+)HLA-DR(-/low) cells correlate with clinical cancer stage and pathological grade in patients with bladder carcinoma. J Int Med Res. 2011;39(4):1381-91.
5. Sun HL, Zhou X, Xue YF, Wang K, Shen YF, Mao JJ, et al. Increased frequency and clinical significance of myeloid-derived suppressor cells in human colorectal carcinoma. World J Gastroentrol. 2012;18(25):3303-09.
6. Srivastava MK, Zhu L, Harris-White M, Kar U, Huang M, Johnson MF, et al. Myeloid suppressor cell depletion augments antitumor activity lung cancer. PloS One. 2012;7(7):e40677, http://dx.doi.org/10.1371/journal.pone.0040677.
7. Lu T, Ramakrishnan R, Altiok S, Youn JI, Cheng P, Celis E, et al. Tumor-infiltrating myeloid cells induce tumor cell resistance to cytotoxic T cells in mice. J Clin Invest. 2011;121(10):4015-29, http://dx.doi.org/10.1172/JCI45862.
8. Salinas NR, Lopes CT, Palma PV, Oshima CT, Bueno V. Lung tumor development in the presence of sphingosine 1-phosphate agonist FTY720. Pathol Oncol Res. 2009;15(5):549-54, http://dx.doi.org/10.1007/s12253-009-9152-2.
9. Salinas NR, Oshima CT, Cury PM, Cordeiro JA, Bueno V. FTY720 and lung tumor development. Int Immunopharmacol. 2009;9(6):689-93, http://dx.doi.org/10.1016/j.intimp.2008.12.007.
10. Enioutina EY, Bareyan D, Daynes RA. A role for immature myeloid cells in immune senescence. J Immunol. 2011;186(2):697-707, http://dx.doi.org/10.4049/jimmunol.1002987.
11. Peddareddigari VG, Wang D, Dubois RN. The tumor microenvironment in colorectal carcinogenesis. Cancer Microenviron. 2010:3(1):149-66, http://dx.doi.org/10.1007/s12307-010-0038-3.
12. Kalluri R, Zeisberg M. Fibroblasts in cancer. Nat Rev Cancer. 2006;6(5):392-401, http://dx.doi.org/10.1038/nrc1877.
13. Ostman A, Augsten M. Cancer-associated fibroblasts and tumor growth-bystanders turning into key players. Curr Opin Genet Dev. 2009;19(1):67-73, http://dx.doi.org/10.1016/j.gde.2009.01.003.
14. Horie M, Saito A, Mikami Y, Ohshima M, Morishita Y, Nakajima J, et al. Characterization of human lung cancer-associated fibroblasts in three-dimensional in vitro co-culture model. Biochem Biophys Res Commun. 2012;423(1):158-63, http://dx.doi.org/10.1016/j.bbrc.2012.05.104.
15. Nazareth MR, Broderick L, Simpson-Abelson MR, Kelleher RJ, Yokota SJ, Bankert RB. Characterization of human lung tumor-associated fibroblasts and their ability to modulate the activation of tumor-associated T cells. J Immunol. 2007;178(9):5552-62.

16. Broderick LA, Bankert RB. Membrane-associated TGF-β1 inhibits human memory T cell signaling in malignant and nonmalignant inflammatory microenvironments. J Immunol. 2006;177(5):3082-8.
17. Bunt SK, Clements VK, Hanson EM, Sinha P, Ostrand-Rosenberg S. Inflammation enhances myeloid-derived suppressor cell cross-talk by signaling through Toll-like receptor 4. Leukoc Biol. 2009;85(6):996-1004, http://dx.doi.org/10.1189/jlb.0708446.
18. Ahmed A, Wang JH, Redmond HP. Silencing of TLR4 increases tumor progression and lung metastasis in a murine model of breast cancer. Ann Surg Oncol. 2012 Aug 14. [Epub ahead of print].
19. Sumida K, Wakita D, Narita Y, Masuko K, Terada S, Watanabe K, et al. Anti-IL-6 receptor mAb eliminates myeloid-derived suppressor cells and inhibits tumor growth by enhancing T-cell responses. Eur J Immunol. 2012;42(8):2060-72.
20. Gabitass RF, Annels NE, Stocken DD, Pandha HA, Middleton GW. Elevated myeloid-derived suppressor cells in pancreatic, esophageal ad gastric cancer are an independent prognostic factor and associated with significant elevation of Th2 cytokine interleukin-13. Cancer Immunol Immunother. 2011;60(10):1419-30, http://dx.doi.org/10.1007/s00262-011-1028-0.
21. Mundy-Bosse BL, Young GS, Bauer T, Binkley E, Bloomston M, Bill MA et al. Distinct myeloid suppressor cells subsets correlate with plasma IL-6 and IL-10 and reduced interferon-alpha signaling in CD4+T cells from patients with GI malignancy. Cancer Immunol Immunother. 2011;60(9):1269-79, http://dx.doi.org/10.1007/s00262-011-1029-z.
22. Cheng YX, Qi XY, Huang JL, Hu M, Zhou LM, Li BS, Xu XX. Toll-like receptor 4 signaling promotes the immunosuppressive cytokine production of human cervival cancer. Eur J Gynaecol Oncol. 2012;33(3):291-4.
23. Bierie B, Moses HL. Transforming growth factor beta (TGF-β) and inflammation in cancer. Cytokine Growth Factor Rev. 2010;21(1):49-59, http://dx.doi.org/10.1016/j.cytogfr.2009.11.008.
24. Li Z, Pang Y, Gara SK, Achyut BR, Heger C, Goldsmith PK, et al. Gr-11 CD11-b cells are responsible for tumor promoting effect of TGF-β in breast cancer progression. Int J Cancer. 2012;131(11):2584-95.